Validation of a coupled FE-BE model of a masonry building with in-situ measurements

Tsouvalas, Apostolos; De Oliveira Barbosa, João; Lourens, Eliz-Mari

Important note
To cite this publication, please use the final published version (if applicable).
Please check the document version above.

VALIDATION OF A COUPLED FE-BE MODEL OF A MASONRY BUILDING WITH IN-SITU MEASUREMENTS

A. Tsouvalas[1], J. De Oliveira Barbosa[2], E. Lourens[3]

[1] *Assistant Professor, Delft University of Technology, Faculty of Civil Engineering and Geosciences, Department of Structural Engineering, Stevinweg 1, Delft, Netherlands, A.Tsouvalas@tudelft.nl*

[2] *Researcher, Delft University of Technology, Faculty of Civil Engineering and Geosciences, Department of Hydraulic Engineering, Stevinweg 1, Delft, Netherlands, J.M.DeOliveiraBarbosa@tudelft.nl*

[3] *Assistant Professor, Delft University of Technology, Faculty of Civil Engineering and Geosciences, Department of Hydraulic Engineering, Stevinweg 1, Delft, Netherlands, E.Lourens@tudelft.nl*

Abstract

Earthquakes induced by the gas extraction is a problem of serious concern in the northern part of The Netherlands. The earthquakes recorded to date can be classified as minor based on their maximum local magnitude (M_L=3.6). However, (i) their shallow focus, (ii) the special *in-situ* soft soil conditions and (iii) the fact the building stock in the region consists primarily of unreinforced masonry, requires some special attention. For this reason, several studies are initiated to investigate the vulnerability of the masonry structures to withstand earthquakes of minor to moderate magnitudes. This paper discusses a detailed study of a masonry school in the region. A coupled finite element-boundary element (FE-BE) model is developed to study the linear dynamic response of the structure to induced seismicity. The structural part, i.e. the masonry building, is modelled using finite elements whereas the soil is described by boundary elements. The modelling of the layered soil medium using boundary elements reduces the computational demands and avoids the need to incorporate non-reflecting boundaries since the radiation condition at infinity is satisfied in an exact manner. This is particularly important for the relatively long wavelengths associated with the low seismic frequencies. The coupled FE-BE model is validated with a full scale *in-situ* experiment in which the structure is set into motion by a vibratory device (*shaker*) which is placed close to the building. To serve this purpose, a special *shaker* was chosen able to extract significant amplitudes in the frequency range between 2-10Hz, which is considered to be relevant for the shallow-focus earthquakes in the region. The dynamic behaviour of the structure, i.e. natural frequencies and modal shapes, is first identified based on ambient vibration measurements. Subsequently, model predictions based on monochromatic ground excitation were compared with *in-situ* measurements for validation purposes. It is shown that the coupled FE-BE model is capable of predicting the dynamic response of the actual system for a wide range of frequencies. Finally, the effects of soft soil-structure interaction and the vibrational characteristics of the structure are investigated for a wide range of frequencies.

Keywords: masonry building; finite element method; boundary element method; seismic motion; soil-structure interaction

1. Introduction

An acceleration record provided by a seismograph in a record station does not account for the presence of buildings, i.e. it corresponds to the situation in which the ground's surface is free of tractions (free field ground motion). When a similar wave field reaches a building (incident field), the latter will interact with soil through the foundation blocks, thus resulting in a motion of the foundations which can be significantly different from the free-field motion of the ground [1]. The incorporation of the recorded motions directly at the foundation level of the building may lead to conservative seismic hazard assessments[1]. To account for the alterations in the incident displacement field, soil-structure interaction needs to be properly considered in the numerical model of the structure.

It is well-known that the seismic response of a flexibly-supported structure will differ in several ways from the one in which the structure is founded on a rigid ground and subjected to an identical free-field excitation. In earthquake engineering, it is customary to replace soil by equivalent linear springs[2] when soil-structure interaction needs to be considered. Empirical equations are used to define the constants of these springs, and then seismic motion is usually prescribed at the free ends of the springs in order to simulate the incoming seismic motion. Since no dissipation mechanism is introduced in this procedure (apart for the internal damping in the building), there is no energy radiation from the building to the soil, and thus the predictions may be very conservative. Moreover, the springs react in a local manner and therefore the stress distribution beneath the foundation blocks is not predicted accurately. Finally, the inclusion of springs can contain no information about the cut-off frequencies of the soil, and so amplification of energy at these particular frequencies is often overlooked.

The following simple example is used here to illustrate the differences between the responses of a system with and without consideration of soil-structure interaction (SSI). The example consists of a rigid mass supported by a spring and a dashpot, which is subjected to an input motion (incident wave field). In the case in which the soil is absent, the motion is prescribed at the free ends of spring and dashpot. In the opposing scenario, the same motion reaches a massless and rigid foundation (with predefined dimensions of 1x1 m^2), which is connected to the spring-damper-mass system. The foundation rests on a homogenous half-space with mass density 1900 kg/m^3, shear wave speed 100 m/s, and Poison's ratio 0.25. The results are compared as function of the natural period of the single degree of freedom (SDOF) oscillator, percentage of the critical damping, and mass of the oscillatory system (this last value is relevant only for the SSI scenario). The input motion is chosen arbitrarily and is depicted in Fig.1a, while the total accelerations of the mass are compared in Fig.1b and Fig.1c for critical damping ratios of 1% and 5%, respectively. It is evident that soil influences significantly the response spectrum of the SDOF system in the following manner: (i) the differences are more pronounced at short periods (high frequencies); (ii) the differences are larger for heavier structures and low-damped systems; (iii) the comparison in Fig.1 also suggests that the application of the seismic motion directly on the base of the spring (thus disregarding the SSI contribution) may lead to overestimation of the structural response, namely because the great majority of natural frequencies of structures are above 2Hz, a range in which the differences are more pronounced for relatively heavy and low-damped structures.

As can be seen, even for this very simple structure (SDOF system) significant differences may occur in the response with and without consideration of SSI phenomena. In the coming sections, we elaborate further on this issue and we present results for a real case examined in the Groningen province (The Netherlands). The structure of the paper is as follows. In section 2, the FE-BE model is described together with a brief description of the solution method. In section 3, the experimental setup is discussed and the comparison of model

---

[1] There are also cases in which the consideration of Soil-Structure interaction (SSI) can yield adverse effects due to soil amplification phenomena in soft soil deposits overlying a very stiff soil layer or a bedrock. In such cases the incorporation of SSI for the predictions of the structural response is mandatory according to Eurocode (EN1998-5).

[2] The representation of the soil reaction by means of linear springs (the Winkler foundation model, for example) often gives good results in such engineering fields as railway and wind engineering, in which the load does not come from the soil. In the earthquake applications, especially in the areas of soft soil, somewhat more sophisticated approach is advisable.

predictions and measurements is presented. Finally, section 4, discusses the main outcome of this paper and the need for further work on the subject.
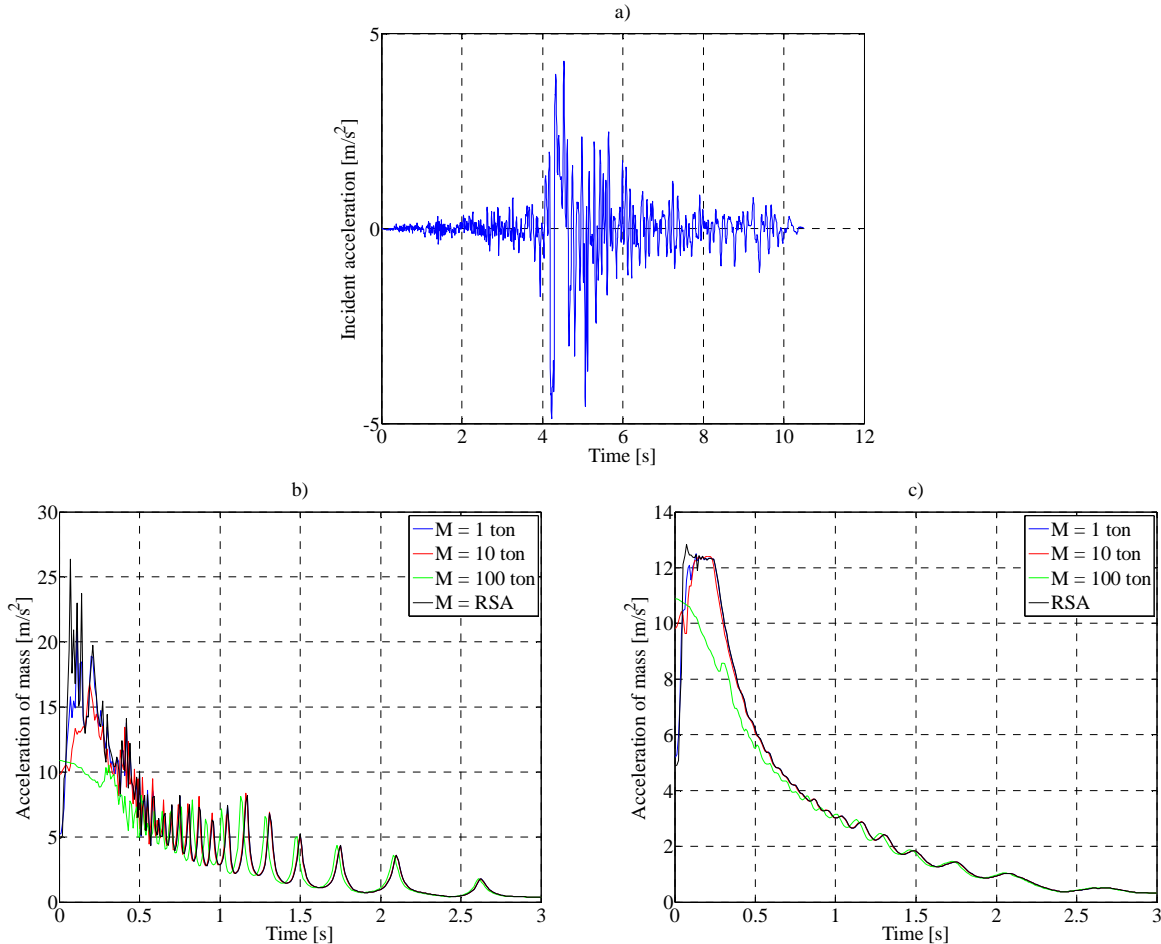

Fig. 1 – a) Input accelerations, b) acceleration responses (1% of critical damping), c) acceleration responses (5% of critical damping). RSA corresponds to the case in which the ground motion is applied directly at the base of the SDOF system (no soil-structure interaction).

2. Model description

As discussed previously, one of the simplest ways to incorporate SSI in an analysis is to include linear springs below the foundation and then to prescribe the motion at the free ends of those springs. Nonetheless, such simplified procedure has several disadvantages even when one is able to predict the spring constants with sufficient accuracy. In general, the reaction of soil is non-local and the stress distribution beneath the foundation blocks depends on the incident, refracted and reflected wave fields which cannot be accounted for by point-wise reacting springs (local springs). More accurate ways of the soil modelling consider the unboundedness of soil (at least up to a certain extent) and treat it as a three-dimensional layered continuum. To this end, the following methods are very often used in practise:

- Solid finite elements (FE) are placed beneath the structure and form an integral part of the FE model. These are usually avoided in practice due to computational restrictions. In addition, they require the truncation of the infinite soil domain; a task which is computationally demanding (and in fact inaccurate) for fields consisting of multiple frequencies and relatively long wavelengths (in this case a large FE domain is required);

- Boundary Elements (BE) [2] are used for the modelling of the unbounded soil domain. which require only the discretization of the surfaces in contact with the structure, thus saving computational resources and time. In addition, they satisfy the radiation condition at infinity in an exact sense and remove the need for truncation of the physical domain altogether.

In the calculations presented herein the soil is modelled with boundary elements and the structure with finite elements. This yields a so-called coupled FE-BE model as described below.

2.1 Boundary element method

In a nutshell, using BEM, the soil flexibility is obtained by applying unit forces at each discretized node and calculating the inflicted displacements at the remaining nodes (Green's functions). This flexibility matrix is frequency dependent, which implies repeating the procedure as many times as the number of frequencies needed for the analysis. The soil stiffness matrix is thereafter calculated by inverting the flexibility matrices. For the calculation of the Green's functions (and soil flexibility matrix), some model of the soil has to be assumed. In this work the Thin Layer Method (TLM) is used [3]. Very briefly, the TLM resembles closely the FEM, but requires discretization only in the vertical direction. The horizontal directions are treated analytically, which provides more accurate results and avoids the truncation of domain [4,5].

In order to create a TLM model, it suffices to define the soil stratification and the material properties of each layer, namely the density, the Poisson's ratio, the shear wave speed, and the internal (material) damping. Damping is accounted for by considering complex wave speeds, according to the expression

$$\overline{C_{P,S}} = C_{P,S}\sqrt{1 + 2i\xi_{P,S}}$$

The subscripts P and S refer to the compressional and shear waves, respectively, $\xi_{P,S}$ refers to the internal material damping, and $C_{P,S}$ refer to the corresponding real wavespeeds.

After obtaining the stiffness matrix of the soil $\mathbf{K^{Soil}}$ (calculated with the TLM-BEM procedure) and the dynamic stiffness matrix of the structure $\mathbf{K^{Struc}}$ (frequency dependent combination of the mass $\mathbf{M}$, damping $\mathbf{C}$ and stiffness $\mathbf{K}$ matrices provided by FEM software: $\mathbf{K^{Struc}} = -\omega^2 \mathbf{M} + i\,\omega\,\mathbf{C} + \mathbf{K}$), the two domains are coupled. The forces acting on the structure from the soil must be in equilibrium with the forces exerted from the structure on the soil, i.e. $\mathbf{F^{Struc}} + \mathbf{F^{Soil}} = \mathbf{0}$, while the displacements on the structure must be compatible with the soil displacements induced by the forces plus the incident displacement field, i.e. $\mathbf{u^{Struc}} = \mathbf{u^{Soil}}\,\mathbf{F^{Soil}} + \mathbf{u^{inc}}$. These two conditions, together with the governing equations of the two domains, result in the following system of equations:

$$\begin{cases} \begin{bmatrix} \mathbf{K}_{I,I}^{Struct} & \mathbf{K}_{I,II}^{Struct} \\ \mathbf{K}_{II,I}^{Struct} & \mathbf{K}_{II,II}^{Struct} \end{bmatrix} \begin{bmatrix} \mathbf{u}_I^{Struct} \\ \mathbf{u}_{II}^{Struct} \end{bmatrix} = \begin{bmatrix} \mathbf{0} \\ \mathbf{F}^{Struct} \end{bmatrix} \\ \mathbf{K}^{Soil}\mathbf{u}^{Soil} = \mathbf{F}^{Soil} \\ \mathbf{u}^{Struct} = \mathbf{u}^{Soil} + \mathbf{u}^{inc} \\ \mathbf{F}^{Struct} + \mathbf{F}^{Soil} = \mathbf{0} \end{cases}$$

(1)

which when simplified, result in the final system of equations[3]

$$\begin{bmatrix} \mathbf{K}_{I,I}^{Struct} & \mathbf{K}_{I,II}^{Struct} \\ \mathbf{K}_{II,I}^{Struct} & \mathbf{K}_{II,II}^{Struct} + \mathbf{K}^{Soil} \end{bmatrix} \begin{bmatrix} \mathbf{u}_I^{Struct} \\ \mathbf{u}_{II}^{Struct} \end{bmatrix} = \begin{bmatrix} \mathbf{0} \\ \mathbf{K}^{Soil}\mathbf{u}^{inc} \end{bmatrix}$$

(2)

Equation (2) is closely related to the equations obtained with the simplified approach in which linear springs are used. The differences are in the stiffness matrices of the soil, which in the simplified procedure are diagonal, frequency independent and real-valued. In the BE model these matrices are fully populated, frequency-dependent and complex-valued. The real part of the soil stiffness is related to the added stiffness and mass of the soil beneath the foundation (in the case of linear springs, only the stiffness can be considered). The imaginary

---

[3] For convenience, the equations of the structure were divided into two parts, the first denoted by I and that represents the degrees of freedom that are not in contact with the soil, and the second denoted by II and that represents the DOFs in the SSI region.

part of the soil stiffness is related to energy dissipation, i.e. energy exchange between the structure and the soil, as well as material dissipation. The non-diagonal structure of $\mathbf{K}^{\mathbf{Soil}}$ is associated with the physical connection between different nodes of the foundations (non-local soil reaction). The frequency dependency is an intrinsic property of the soil, which is also observed in the dynamic stiffness matrix of the structure. A more detailed description of the method is given in [6,7] and is omitted here for the sake of brevity.

2.2 Soil properties

The soil is modelled hereafter as a viscoelastic layered half-space. To account for the saturation of the layers, and therefore the change in compressibility, the Poisson ratio is assumed constant with depth and very close to 0.5 (the Poisson's ratio was set equal to 0.495 in all layers). The layered profile for the soil was decided based on the results of CPT tests that are available in the DINO locket database [8]. The values of the shear wave speeds V_s of the various layers were based on CPT tests via empirical equations. Several equations are available in the literature; in this study, the Robertson equations [9] are chosen because they are more suitable for the ground conditions in Groningen. The depth dependent shear waves speeds estimated based on the CPT tests are compiled in Fig.2. Together with the estimated lines, same limiting scenarios are presented, namely a soft scenario (left green line), an average scenario (red line) and a stiff scenario (right green line).
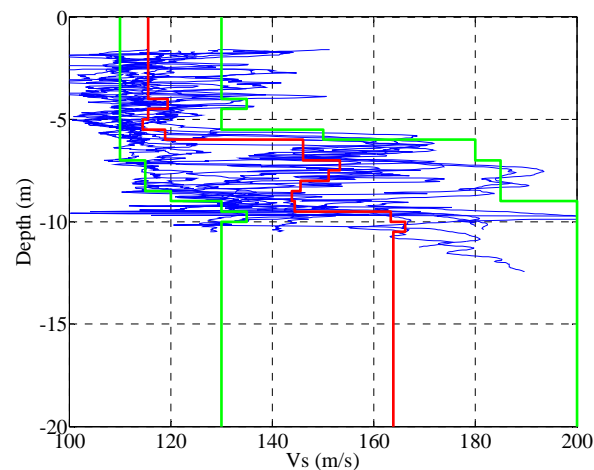

Fig. 2 – Shear wave velocities of the soil. Blue lines correspond to the CPT tests and Robertson equations; outer left green line = softest scenario; red line = average scenario; outer right green line = stiffest scenario

Regarding the remaining properties of the soil (mass density and internal damping), no relevant information for the definition of these variables was available at the time of the present study. Therefore, reasonable average values from similar cases were adopted. A mass density of 1900 kg/m3 and an internal damping of $\xi_S = \xi_P = 0.02$ were used. The effect of internal damping was not examined in depth but it is to be expected that in this low frequency regime, the soil damping is dominated by radiation of waves rather than by energy absorption. Three TLM models for the soil were created, one for each of the profiles depicted in Fig.2. The TLM models contain elastic regions up to 12 meters depth divided into thin-layers of 10cm each and of quadratic expansion. This gives a total of 240 nodes in the TLM models, and about 100 thin-layer interfaces per wavelength at the highest frequency included in the analyses (20 Hz). Twenty thin-layers per wavelength are enough to reduce to negligible the errors due to vertical discretization. Perfectly matched layers (PML) are added to the 12 m deep elastic region in order to simulate the lower half-space [10].

5

2.3 Structural model (FEM) and SSI surface model (BEM)

The FEM model used to simulate the building is composed mainly of beam and shell elements as shown in Fig.3 and is built in FE software TNO Diana [11]. It consists of masonry walls modelled with shell elements, roof beams modelled with beam elements and foundation piles (shown at the part of the building at the right of the figure) which are also modelled as beam elements.
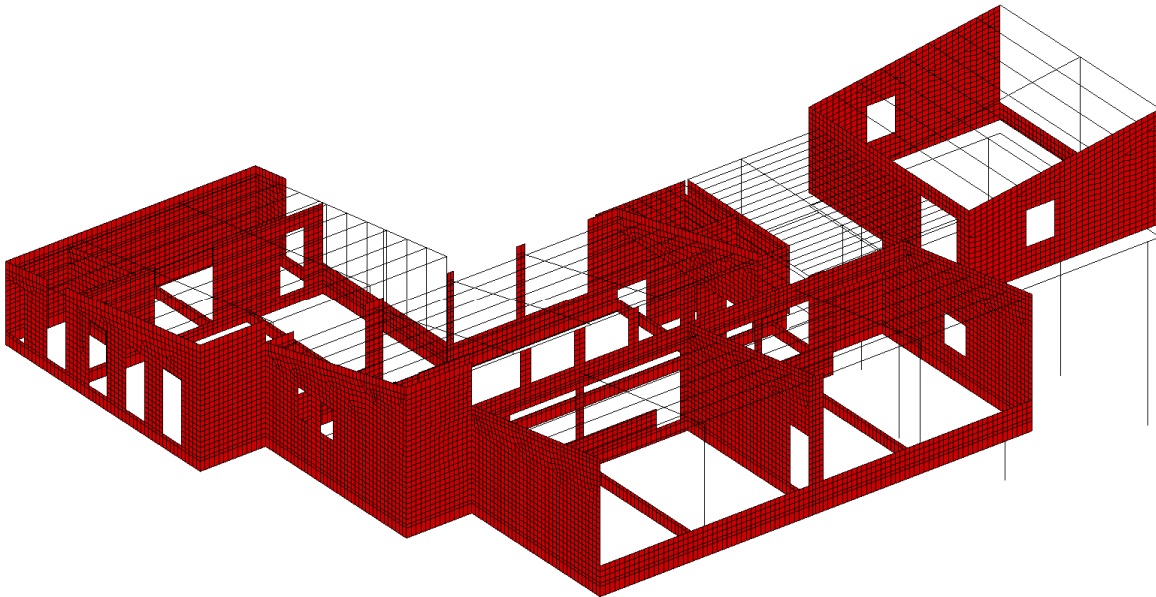
Fig. 3 – Finite element model of the structure

In Fig.3, the mesh of the FEM model of the structure is shown (the number of degrees of freedom is approximately 100.000). The structural damping is accounted for by means of the Rayleigh damping matrix. The mass proportional and stiffness proportional coefficients are chosen such that the equivalent modal damping at the frequencies 1 Hz and 10 Hz is equal to 5%.

Regarding the BEM model used to describe the surfaces of the soil interacting with the structure, it was defined in such a way that for each beam element of the foundation or for each node of the piles there is one boundary element. In total there are 1593 boundary element nodes. The BEM mesh is shown in Fig.4. Please note that the width associated with distinct BEM elements is not necessarily the same. Such is so because the beam elements of the foundation do not all have the same dimensions.
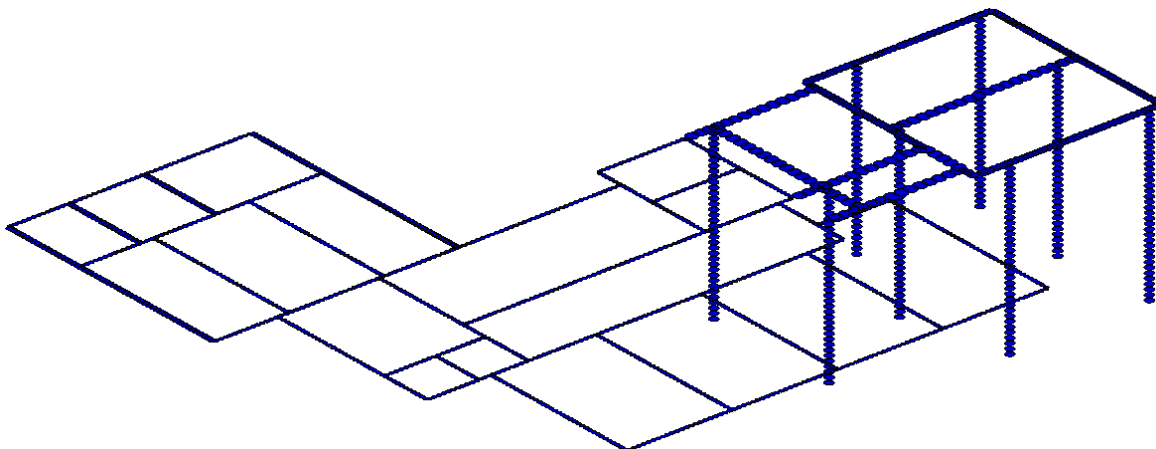
Fig. 4 – Boundary element mesh of the soil

3. Experiment and model validation

The present section describes the in situ dynamic tests that were performed at the school masonry building in the north of the Netherlands in February 2015. The aim of the test campaign was twofold. A first objective was to reduce the modelling uncertainty resulting from inaccurate or uncertain information on the various parameters used to construct the model. These include, but are not limited to, the material and geometric properties of the structure, the fixity of various structural connections, the stiffness of the supporting soil, and the assumed boundary conditions. The second aim was to validate the accuracy of the model by comparing the measured vibration levels in the building, caused by an *a priori* defined force input exerted by the shaker in the soil medium, to those calculated by the model. To reach these objectives, two types of tests were performed in the full-scale structure, namely passive (or ambient vibration testing), and active source experiments with a low-frequency seismic vibrator. In section 3.1, the former experiment is discussed whereas in section 3.2, the results of the forced vibrations experiment are presented.

3.1 Ambient vibration measurements and modal analysis

The experimental set up is shown in Fig.5 in which the tested masonry building is shown together with the shaker positioned at a certain distance from the building. Given the limited number of seismometers available, tests were performed in eight different set up's, roughly corresponding to eight different walls of the school building as indicated in Fig.6. A choice was made to exclude measurements on the part of the building founded on piles, due to time restrictions.

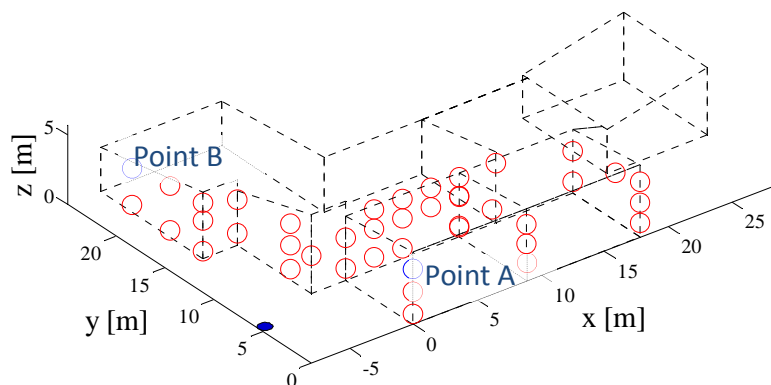Fig. 5 – Experimental setup with the shaker used in the experiment

Fig. 6 – Layout of the experimental configurations related to the eight main walls of the building. Sensor locations in red colour and shaker position in blue colour on the ground surface (section 3.2)

During each set up, velocities were measured using eight tri-axial seismometers (24 channels) at a sampling frequency of 200Hz. The recording length for the ambient testing was about 20 minutes. Three reference sensors remained stationary during all set up's; five were moved occasionally from wall to wall (Fig.6). Each seismometer had its own data recording system, powered by batteries. Fig.7 below shows the seismometers and seismic recorders used in the experiment.
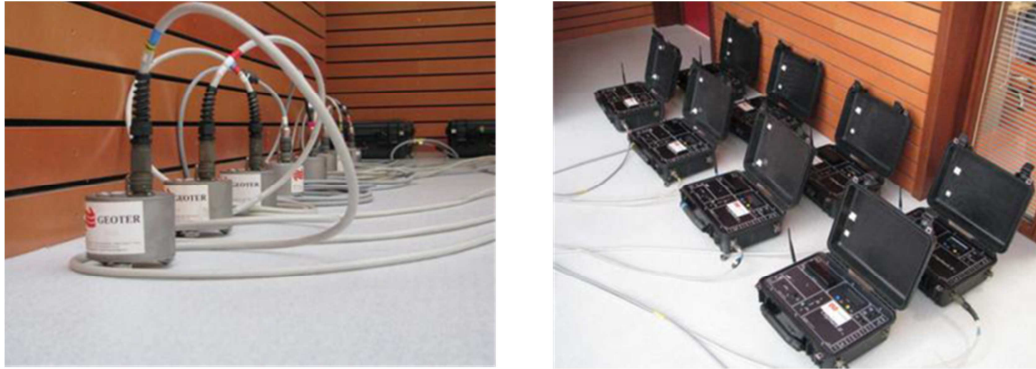

Fig. 7 – Seismometers (left) and seismic recorders (right)

To facilitate the extraction of the desired dynamic information using as few sensors as possible, the measurement locations were chosen based on the results of a preliminary modal analysis of the building and the expected modal shapes of the structure. A typical vibration signal measured during the ambient testing (velocity in the x direction for position 202 during set up 1) is presented in Fig.8 in both the time and the frequency domain. As can be seen, the measured natural vibrations all contained some disturbances due to, for instance, the inhabitants walking through the building. For the operational modal analysis described in the this section, the signal windows without any local perturbations have to be isolated first.
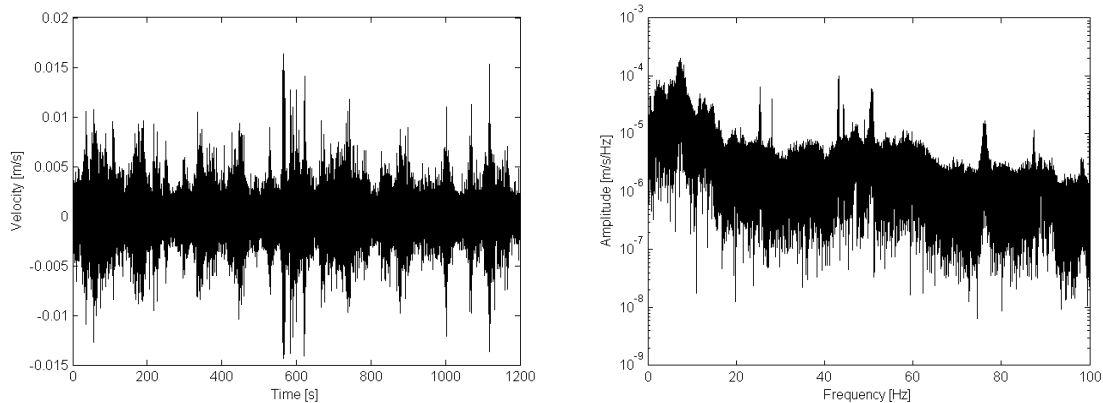

Fig. 8 – Time history (left) and frequency spectrum (right) of the horizontal component of velocity measured at point 202 during set up 1.

Ambient or passive vibration testing relies on the natural vibrations existing at every site to identify certain properties of a structure and/or the soil. If the properties to be identified are the modal parameters of a structure (natural frequencies, mode shapes), one speaks of operational modal analysis [12,13]. In order to extract modal properties using these so-called output-only techniques, certain assumptions are made about the dynamic characteristics of the input forces, e.g. that these can be modelled as white noise stochastic processes having broadband spectra.

The modal parameter extraction of the school building was performed using frequency domain decomposition [14]. This technique belongs to the family of Principal Component Analysis (PCA) methods [15,16], which relies on the property of the Singular Value Decomposition (SVD) to represent a set of functions

as a product of weighting factors and independent linear contributions. First, the spectral matrices for all 144 time series measured at the school are estimated. These frequency-dependent matrices collect in their diagonal and off-diagonal terms, respectively, the power spectral densities and cross-spectral densities of all measured time series. In a second step, the spectral matrices are decomposed into a number of linearly independent orthogonal components using the SVD:

$$\tilde{\mathbf{S}}_{dd}(\omega) = \mathbf{U}\boldsymbol{\Sigma}\mathbf{U}^{\mathrm{T}} \tag{3}$$

where $\tilde{\mathbf{S}}_{dd}(\omega)$ signifies the spectral matrix, $\mathbf{U}$ collects as columns its orthogonal components (the *singular vectors*), and $\boldsymbol{\Sigma}$ is a diagonal matrix containing the weighting factors for each of the orthogonal components in $\mathbf{U}$. A selection of these weigting factors or *singular values* is plotted in Fig.9 for the frequency range 0 - 6 Hz. These singular values indicate how many orthogonal components are contributing to the measured data at each frequency. The orthogonal components themselves can be extracted from the singular vector matrix $\mathbf{U}$ at the frequency of interest. Considering the singular vector spectrum presented in Fig. 9, the following conclusions can be drawn:

- A dynamic amplification occurs around 0.5 Hz. Since all distinguishable orthogonal components in the data experience a similar amplification in this frequency range, it can be concluded that the amplification is not caused by a structural resonance, but by an amplification in the exerted excitation. This excitation around 0.5 Hz is most likely originating from the soil (being a soil mode);

- The next amplification occurs shortly after 2 Hz. Here a single orthogonal component is clearly contributing more to the measured data than the others, indicating a structural resonance;

- The same conclusion as above can be drawn from the amplification around 5 Hz.
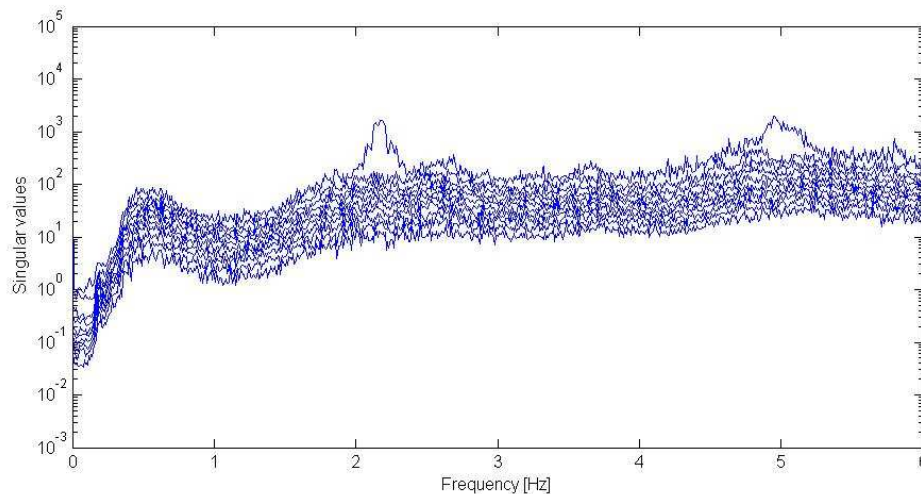

Fig. 9 – Singular value spectrum of the PSD's of all sensor data combined

The singular value spectrum thus provides an intuitive means of not only identifying structural mode shapes but also distinguishing between dynamic amplification due to external excitation as opposed to internal resonances of the structure. As such, the frequency domain decomposition technique can be considered as a SVD-based extension of the early peak-picking method, thereby resolving issues related to identification in the presence of harmonics as well as mode multiplicity problems [17]. Applying the FDD to the ambient data gathered, resulted in the identification of 14 vibration modes, 13 of which are identified as structural modes and one soil mode. A 3-D view of the singular vector or mode corresponding to the soil amplification at 0.5 Hz is shown in Fig.10 (left) together with the first structural mode (right).

The analysis has concluded that the majority of identified eigenvectors involve local vibrations, with often only a few walls contributing to the response. This can significantly complicate the model updating process. As a final comment, it is mentioned that the mode shapes identified by means of the FDD on the basis of output-only data inherently include the effects of soil-structure interaction. Because soil effects are dependent on the frequency as well as amplitude of the applied excitation, the identified shapes are subject to change in situations where the order of magnitude or frequency content of the excitation change significantly. This effect has been

illustrated on the *Polymylos* bridge in Greece where output-only modal identification was performed using ambient as well as earthquake excitation [18].
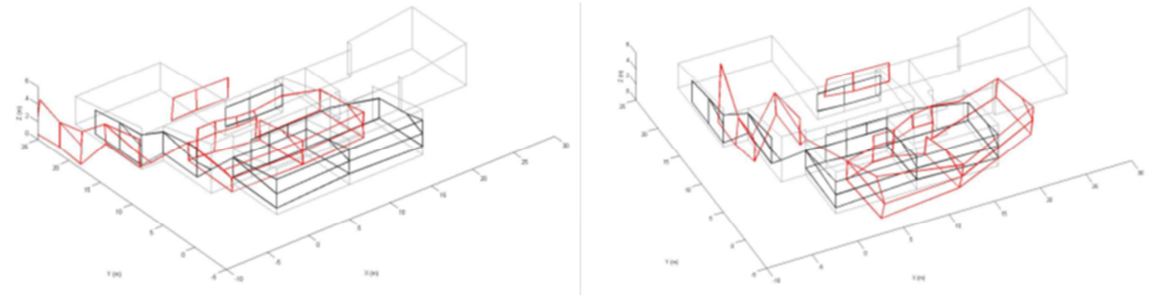

Fig. 10 – Identified mode 1 at 0.5 Hz (left) and mode 2 at 2.1 Hz (right)

3.2 Forced vibrations and FE-BE model validation

In the second part of the experiment, the response of the building is monitored when the latter is excited by a well-controlled source mechanism. In this case, the school was excited by a heavy shaker (with controlled frequencies and amplitudes), and the velocities at several points in the structure were measured (Fig.5). Important to mention is that there was no direct contact between shaker and building, i.e. the excitation was transmitted solely through the soil. Thus, a good correspondence between the predicted and measured response would imply that not only the FE model is representative of the building, but also the BE-FE procedure is appropriate to model the linear interaction between the soil and the structure.

Due to the limitation on the number of seismic recorders, the experiments had to be divided into several steps. At each step, a given wall was monitored due to environmental noise/loads (section 3.1). After that, the forced experiment was carried out meaning that the shaker was turned on in order to excite the building, and the induced vibrations were recorded at the same points. The shaker was operated at distinct frequencies and amplitudes ranging from 2 Hz to 10 Hz and from 2kN to 6 kN, respectively. For each frequency-amplitude set, the induced velocities were recorded twice for periods of one minute. For the lowest frequency (2 Hz), one minute corresponds to 120 cycles, which are considered sufficient to reach the steady-state regime. In total, seven walls of the school were tested during the operation of the shaker. The position of the measuring points are indicated in Fig.6 with red hollow circles, while the position of the shaker is indicated with a blue filled circle. There were two additional measuring points (points A and B) that were not changed through the measurement campaign. These two points are represented with hollow blue circles.

To calculate the frequency response function ($FRF_{x,y,z}$) based on the time history of velocities, the time records are passed through a low-pass filter and a high-pass filter in order to remove the contributions of the frequencies below $f=f_0-1$ and, $f=f_0+1$ with f_0 being the induced frequency. Thereafter, the oscillating amplitude of velocities $V_{x,y,z}$ is obtained by averaging the local maxima observed between 10 and 50 seconds of the filtered time history, i.e.:

$$FRF_{x,y,z} = \frac{\bar{V}_{x,y,z}}{2\pi f_0 A_0}$$

(4)

where A_0 is the amplitude of the force induced by the shaker as described above.

The FRFs of points A are shown in Fig.11. Each tested frequency contains 14 data points since each set up (each wall) is tested twice for each frequency. The measured FRFs are accompanied with the FRFs estimated based on the BE-FE model described in section 2. For point A, the dispersion is insignificant, i.e., for a given frequency, the measured FRFs do not change significantly. Regarding the comparison between measured and predicted FRFs, there is not a perfect match. Nevertheless, the values are of the same order of magnitude and for the frequency 7.5 Hz the correspondence is very good. In all cases, the predicted response is within the same magnitude as the measured response.

Another is shown in Fig.12 for the FRFs in several directions and for one of the walls of the building. Six sensors were used to record the response of this wall. For the horizontal in-plane direction (y), the agreement

between predicted and observed amplitudes is good for the frequencies 4, 5 and 7.5 Hz. For the remaining directions, only for 7.5 Hz the agreement is good (there are some exception at some sensors). In all cases, the amplitudes are of the same order of magnitude. It is interesting to observe that for the frequencies 2 and 3 Hz, all receivers measured approximately the same amplitude of displacements. This suggests that this wall responds as a rigid body, i.e., does not suffer any internal deformation. Similar results were obtained for other wall elements as well and are omitted here for the sake of brevity.
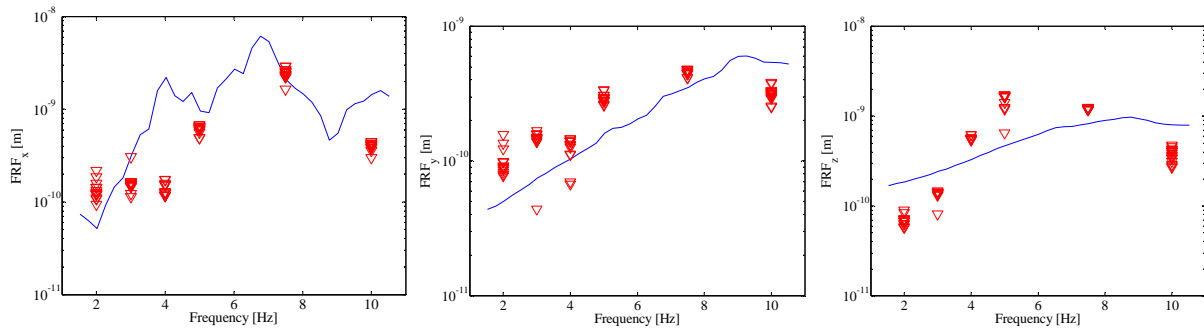
Fig. 11 – FRFs of points A: Red triangles = observed amplitudes; blue line = predicted amplitudes
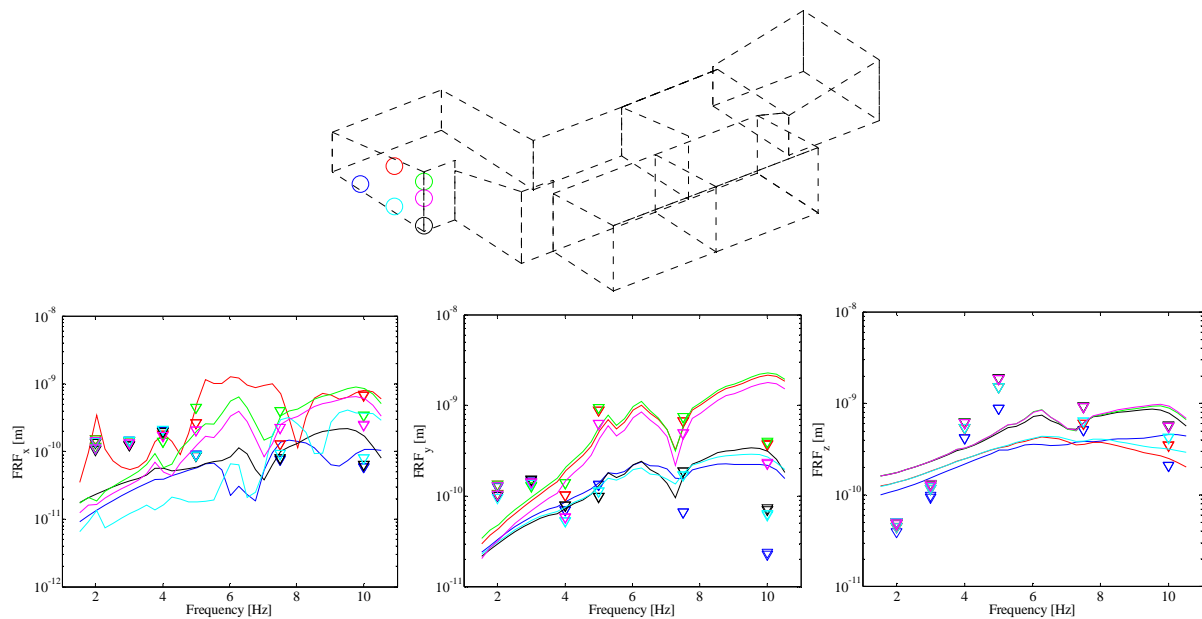
Fig. 12 – Location of sensors and comparison of measured and predicted responses for a single wall. The FRFs of each receiver are represented by the corresponding colour.

4. Conclusions

In this paper an experimental campaign is described. The purpose of this study was to investigate the influence of soil-structure interaction for a specific case and to validate a coupled FE-BE model that was developed. Two measurement set up's are analysed. The first one aimed in the identification of the natural frequencies and modal shapes of the structure. By applying the frequency domain decomposition to the ambient data collected for various walls of the structure, 14 vibration modes were identified, 13 of which were structural modes and one being a soil mode. In the second one, a forced experiment was carried out in which the building was excited via the soil with the use of a specially-designed shaker able to operate at very low frequencies. The measurements were compared to model predictions. The observed and the predicted responses for most of the measuring points

and frequencies were found to be within the same order of magnitude. Given the uncertainty in a large number of parameters in the fully-coupled soil-structure interaction model, the predictions can be considered as reliable. The difference in the displacement field for certain frequencies was limited to ±20%. In the higher frequencies though, differences in the order of 100% were observed. Despite the apparent differences, the FE-BE model is still capable of providing a realistic representation of the response of the actual system to a given input ground motion. It is in fact one of the few models to date, in which a direct comparison of predictions and measurements is illustrated for the case in which the structure is excited through the soil for a number of frequencies relevant to seismic excitations.

5. References

[1] Garcia, J.A. (2008): Soil structure interaction in the analysis and seismic design of reinforced concrete frame buildings. *Proceedings of the fourteenth World Conference on Earthquake Engineering,* Beijing, China, pp 1-9.

[2] Beskos, D.E. (1993): Applications of the Boundary Element Method in Dynamic Soil-Structure Interaction. *Developments in dynamic Soil-Structure Interaction*, Vol **390** of the series NATO ASI Series, pp 61-90.

[3] Kausel, E. (1986): Wave propagation in anisotropic layered media. *International Journal for Numerical Methods in Engineering*, Vol **23**, pp 1567-1578.

[4] Kausel, E. and Peek, R. (1982): Boundary integral method for stratified soils. *MIT Research report R82-50, Department of Civil Engineering*.

[5] Barbosa, J., Kausel, E., Azevedo, A. and Calçada, R. (2013): A 2.5D BEM procedure based on the TLM, *ICOVP 2013*, Lisbon, 9-12 September.

[6] Barbosa, J., Alves Costa, P. and Calçada, R. (2015): Abatement of railway induced vibrations: numerical comparison of trench solutions. *Accepted for publication in Engineering Analysis with Boundary Elements*.

[7] Hussein, M., Hunt, H., Kuo, K., Alves Costa, P. and Barbosa, J. (2014): The use of sub-modelling technique to calculate vibration in buildings from underground railways*, Proceedings of the institution of mechanical engineers Part F: Journal of rapid transit*.

[8] www.dinoloket.nl

[9] Robertson, P.K. (2009): Interpretation of cone penetration tests – a unified approach. *Can. Geotech. J.*, Vol **46**, pp 1337-1355

[10] Barbosa, J., Park, J. and Kausel, E. (2012): Perfectly matched layers in the thin layer method. *Computer methods in applied mechanics and engineering*, Vol **217-220**, pp 262-274

[11] DIANA. Finite Element Code: User's Manual – Release 9.3, TNO Building and Construction, Research: Delft, The Netherlands. 2012.

[12] Reynders, E. (2012). System Identification Methods for (Operational) Modal Analysis: Review and Comparison. *Archives of Computational Methods in Engineering, 19*(1), 51-124.

[13] Peeters, B., & De Roeck, G. (2001). Stochastic System Identification for Operational Modal Analysis: A Review. *Journal of Dynamic Systems, Measurement, and Control, 123*(4), 659-667.

[14] Brincker, R., Zhang, L., & Anderson, P. (2001). Modal identification of output-only systems using frequency domain decomposition. *Smart Materials and Structures 10*, 441-445.

[15] Allemang, R. J., Phillips, A. W., & Allemang, M. R. (2010). Application of Principal Component Analysis Methods to Experimental Structural Dynamics. *Proceedings of the IMAC-XXVIII*. Jacksonville, Florida USA.

[16] Allemang, R., & Brown, D. (1982). A correlation coefficient for modal vector analysis. *Proceedings of the 1st International Modal Analysis Conference*, (pp. 110-116). Orlando, Florida USA.

[17] Bishop, R., & Gladwell, G. (1963). An investigation into the theory of resonance testing. *Philosophical Transactions of the Royal Society of London, 255A*(1055), 241-280.

[18] Ntotsios, E., Karakostas, C., Lekidis, V., Panetsos, P., Nikolaou, I., Papadimitriou, C., et al. (2009). Structural identification of Egnatia Odos bridges based on ambient and earthquake induced vibrations. *Bulletin of Earthquake Engineering, 7*(2), 485-501.